Dump Load Allocation in Islanded Microgrid with Robust Backward\Forward Sweep and MIDACO

Maen Z. Kreishan
Deptartment of Electronic and Electrical Engineering
Brunel University London
Uxbridge UB8 3PH, UK
maen.kreishan@brunel.ac.uk

Ahmed F. Zobaa
Deptartment of Electronic and Electrical Engineering
Brunel University London
Uxbridge UB8 3PH, UK
azobaa@ieee.org

***Abstract*—Dump load (DL) allocation in droop-controlled islanded microgrid (DCIMG) is vital to consume excess generation at off-peak hours and provide voltage and frequency (V-f) support. Furthermore, convergence of load flow (LF) solution is necessary to determine optimal working points of any DCIMG. Proposed in this paper, two LF methods based on the famous backward/forward sweep (BFS): improved special BFS (SBFS-II) and general BFS (GBFS). The former method is based on global voltage variable spread among all distributed generation (DG), while the latter is more general by considering local voltage measurement at each DG. The multi-objective problem of DL allocation in highly penetrated DCIMG to minimize V-f deviations and power losses was investigated using the two LF methods combined with mixed-integer distributed ant colony optimization (MIDACO). The problem was applied to the IEEE-33 bus system, while solutions were subjected to various convergence tests. Results show SBFS-II and GBFS efficacy in calculation time and accuracy of the solution, respectively, for DL allocation problem in DCIMG.**

Keywords— Ant Colony Optimization, Backward/Forward Sweep, Droop Control Islanded Microgrid, Dump Load, Load Flow, Multi-objective Optimization

I. Introduction

Stable and reliable microgrid (MG) operation is vital in facilitating distributed generation (DG) growth with increased reliance on renewable resources. Autonomous MG, often referred to as islanded MG (IMG), has become an area of interest [1]. Furthermore, due to its ease of implementation and reliability for IMG, droop control have gained considerable share of studies that focused on optimal operation of droop-controlled IMG (DCIMG) [1]. Highly penetrated DCIMG has resulted in voltage and frequency (V-f) regulation issues, this was more evident during off-peak hours. This is attributed to the intermittent nature of renewable generation and lower electricity demand. Dump loads (DL) are known to provide adequate power management solution for significant mismatch situations [2]. Nonetheless, few studies have tackled the optimal DL allocation problem to provide V-f support at low load hours in DCIMG framework [2]–[4]. Therefore, more studies are necessary to highlight the importance of DL planning in IMG. The use of efficient and robust load flow (LF) in DCIMG is necessary to predict DCIMG operation, thus, providing sufficient modelling of IMG in optimization studies. As stated by the pivotal work of [5], Jacobean-based LF is not suitable for radial and weakly meshed distribution systems. This is attributed to the high R/X ratio which cause singularity in the Jacobean matrix leading to convergence problems [6]. Therefore, backward/forward sweep (BFS) methods have gained popularity as LF in IMG. As in [7], a direct BFS (DBFS) was proposed to provide suitable solution for DCIMG without relying on the Jacobean matrix. Similarly, a modified BFS (MBFS) was presented in [8] to account for local voltage by DGs in DCIMG, while [9] suggested a nested BFS (NBFS) to enhance the convergence of MBFS. However, ill-conditioned systems with variations in droop setting or generation and load levels degrade the convergence of the forgoing methods and limit the boundary conditions for decision variables of optimization problems. As in [4], stability improvement in highly penetrated MG was achieved by the optimal dump load (DL) allocation using combination of robust LF method called special BFS (SBFS) and the mixed-integer distributed ant colony optimization (MIDACO) algorithm. The use of stochastic optimization techniques to solve non-convex mixed-integer non-linear problems (MINLP) has gained significant interest in many years [1]. Ant colony optimization (ACO) is a well-established metaheuristic that is based on real ants foraging behaviour. On the other hand, the proposed optimization technique in this paper, MIDACO, is based on the extended ACO (ACOmi) [10] mixed with the oracle penalty method (OPM) [11]. The advantage of MIDACO against other multi-objective optimization metaheuristics is the utopia-nadir balance approach to steer the non-dominated search toward the best point on a Pareto-front [12].

In this paper, we highlight the importance of DL allocation to consume excess power during off-peak hours by proposing two LF methods to further enhance MIDACO performance. This is done by finding the optimal DL size and location as well as the optimal droop setting for DGs to minimize V-f deviations and power losses in the IEEE 33-bus islanded system. The first LF method, called improved SBFS (SBFS-II), is based on SBFS [4] with enhanced convergence rate. While the second method, called general BFS (GBFS), employs two dynamic damping factors with a correction vector to offer accurate representation of droop-control with enhanced convergence.

II. Methodolgy

A. Droop Control and SBFS Method

In DCIMG, generation units are typically modelled as inverter-based DG (IBDG), where V-f droop control is facilitated by power electronics. The inverter control system of typical IBDG utilizes the P-f and Q-V droop equations given in (1) and (2), respectively [4]. Such equations influence DGs output active (P_{Gi}) and reactive (Q_{Gi}) power to enable load change following as per IEEE std.1547.7 [13]:

$$f - f_0 = m_{pi}\,(P_{Gi} - P_{Gi0}) \quad (1)$$

$$|V_i| - |V_0| = n_{qi}\,(Q_{Gi} - Q_{Gi0}) \quad (2)$$

where m_{pi} and n_{qi} are active and reactive droop coefficients at bus i, respectively; V_0 and f_0 are the nominal

V - f values, respectively; P_{Gi0} and Q_{Gi0} are active and reactive nominal powers at bus i, respectively. The above droop equations are widely accepted assumption based on the highly inductive DG output impedance [13]. However, generally, the active and reactive IBDG power output might not be decoupled, hence there is a simultaneous relationship between V-f and output power. Therefore, droop equations for IBDG considering complex output impedance in P- V -f and Q- V -f forms are as follows [14]:

$$f - f_0 = m_{pi}\,(P_{Gi} - Q_{Gi}) \quad (3)$$

$$|V_i| - |V_0| = n_{qi}\,(P_{Gi} + Q_{Gi}) \quad (4)$$

Conversely, for sake of simplicity, a constant power load model was adopted for all loads and DL in this study [4]. To account for droop response by DGs the SBFS method was proposed in [4]. SBFS consists of four stages as follows:

1) *Initialization Stage*: The virtual bus (VB), solution to slack bus concept in IMG, was set as bus 1, while $1\angle 0^{\circ}$ p.u. initializes all system voltages V_i with tolerance threshold value $\varepsilon_{Th} = 10^{-8}$ [4].
2) *Backward Sweep*: From known apparent powers S_i and voltages V_i, current injects I_i are calculated, then branch currents B_i are obtained moving backward towards the VB.

$$[\boldsymbol{I_i}] = ([\boldsymbol{S_i}]/\,[\boldsymbol{V_i}])^{*} \quad (5)$$

$$[\boldsymbol{B_i}] = [\boldsymbol{BIBC}][\boldsymbol{I_i}] \quad (6)$$

For n-bus radial system, $[\boldsymbol{BIBC}]$ is the bus injects-branch current matrix of size $n-1$ by $n-1$ as defined in [15], while $[\boldsymbol{I_i}]$ and $[\boldsymbol{B_i}]$ are column vectors of size $n-1$ by 1.

3) *Forward Sweep*: New voltages V_{in} are obtained sweeping away from VB using (7), then convergence is checked using voltage error tolerance (E) as in (8):

$$[\boldsymbol{V_{in}}] = [\boldsymbol{V_1}] - [\boldsymbol{BCBV}][\boldsymbol{B_i}] \quad (7)$$

$$\mathrm{E} = \max\{|V_{in} - V_i|\} \quad (8)$$

where $[\boldsymbol{BCBV}]$ is the branch current and bus voltage matrix as obtained in [4].

4) *The Update Stage*: If $\mathrm{E} < \varepsilon_{Th}$, then system frequency (f) and VB voltage (V_1) are updated as follows:

$$\Delta f = -m_{pT} \cdot (P_{G1} - \Re\{V_1 \cdot B_1^{*}\}) \quad (9)$$

$$\Delta V_1 = -n_{qT} \cdot (Q_{G1} - \Im\{V_1 \cdot B_1^{*}\}) \quad (10)$$

$$f_{c_2+1} = f_{c_2} + \Delta f \quad (11)$$

$$V_{1_{c_2+1}} = V_{1_{c_2}} + \Delta V_1 \quad (12)$$

where m_{pT} and n_{qT} are the system equivalent f and V droop coefficients, respectively [7]; $V_1 \cdot B_1^{*}$ is the total apparent power leaving VB; c_2 is an external iteration counter for SBFS. Subsequently, line impedance Z_i and DG active (P_{Gi}) and reactive (Q_{Gi}) powers are corrected at generating buses before the final verification of convergence when $|\Delta V_1| < \varepsilon_{Th}$.

$$Z_i = R_i + \mathrm{j}\,X_i\left(f_{c_2+1}/f_{c_2}\right) \quad (13)$$

$$P_{Gi} = \Delta f/m_{pi} + P_{Gi0}\;;\; \forall\, i \in \mathcal{GK};\; \mathcal{GK} \subseteq \mathcal{N} \quad (14)$$

$$Q_{Gi} = \Delta V_{in}/n_{qi} + Q_{Gi0}\;;\; \forall\, i \in \mathcal{GK} \quad (15)$$

where $\mathcal{GK}$ and $\mathcal{N}$ are sets of generating buses and all system buses in the IMG, respectively.

B. Improved SBFS Method (SBFS-II)

The proposed improvement to SBFS in this paper is based on the voltage update equation (7) and tolerance equation (8). A major issue with DBFS method is having three loops, viz. update voltage, frequency, and DG powers. This would lead to convergence issues for some il-conditioned problems such as the DL allocation problem proposed in this paper. This issue has been reduced in SBFS where only two loops were considered: internal BFS loop with iteration counter c_1 and power and V-f update loop with iteration counter c_2. The novel extension to SBFS, named as SBFS-II, works by completely removing the internal BFS loop and adopting more rigours convergence check. As it is known, more iterations are required to reduce the voltage error across system ($|\Delta V_{in}| = |V_{in} - V_i|$). Conversely, having a global voltage $|\Delta V_1|$ to update all DG reactive power is advantageous in the sense that additional voltage error across the system $|\Delta V_{in}|$ becomes redundant. Therefore, neglecting $|\Delta V_{in}|$ effect on the solution and taking the second guess of $\boldsymbol{V_{in}}$ will have a huge impact on convergence speed of SBFS-II. This can be obtained as follows:

$$[\boldsymbol{I_i'}] = ([\boldsymbol{S_i}]/\,[\boldsymbol{V_{in}}])^{*} \quad (16)$$

$$[\boldsymbol{B_i'}] = [\boldsymbol{BIBC}][\boldsymbol{I_i'}] \quad (17)$$

$$[\boldsymbol{V_{in}'}] = [\boldsymbol{V_1}] - [\boldsymbol{BCBV}][\boldsymbol{B_i'}] \quad (18)$$

where $\boldsymbol{I_i'}$ and $\boldsymbol{B_i'}$ are, respectively, the current injects and branch currents after another backward sweep. Removing the internal BFS loop is helpful since IMG stability is based on $|\Delta V_1|$ minimization. Similarly, V - f update equations are changed to reflect only one iteration counter (c) for SBFS-II:

$$f_{c+1} = f_c + \Delta f \quad (19)$$

$$V_{1_{c+1}} = V_{1_c} + \Delta V_1 \quad (20)$$

To ensure zero power exchange at the VB and account for $|\Delta V_{in}|$ impact on the solution, the convergence criterion in (8) has been updated as well. Hence, a new voltage error tolerance (E') for the whole system is provided, this ensures all generation mismatches are satisfied at each generating bus.

$$|\Delta V_{in}'| = |V_{in}' - V_{in}| \quad (21)$$

$$\mathrm{E}' = |\Delta V_1| + max\{|\Delta V_{in}'|\} \quad (22)$$

C. General BFS Method (GBFS)

The reactive power update in global voltage BFS-based LF methods, such as DBFS and SBFS, requires the existence of good communication between DGs and an MG central controller (MGCC). However, as in many IMG, communication might be weak or prone to delays, hence the need for LF that accounts for local voltage measurements of DGs without relying heavily on communication. In that regard, the proposed second LF method provides a different update to reactive power in (15) by considering local bus voltage and DG droop value. Likewise, reflection of the nominal voltage (V_0) recovery by individual DGs is given as follows:

$$Q_{Gi} = (|V_{in}| - |V_0|)/n_{qi} + Q_{Gi0}\;;\; \forall\, i \in \mathcal{GK} \quad (23)$$

So far, the proposed reactive power update does not differ from that suggested in other local voltage BFS-based LF methods, such as MBFS [8] and NBFS [9]. However, the novel extension of this method is the introduction of P- V -f and Q- V -f equations to account for the complex impedance found at IBDG output in highly resistive distribution line.

$$P_{Gi} = \tfrac{1}{2}\left((|V_{in}| - |V_0|)/n_{qi} + \Delta f/m_{pi}\right);\; \forall\, i \in \mathcal{GK} \quad (24)$$

$$Q_{Gi} = \tfrac{1}{2}\left((|V_{in}| - |V_0|)/n_{qi} - \Delta f/m_{pi}\right);\; \forall\, i \in \mathcal{GK} \quad (25)$$

Furthermore, poor reactive power sharing, unequal line impedance, and lower droop values will lead to convergence

issues in LF solution. Hence, as another extension of GBFS, we propose using two dynamic damping factors ζ_1 and ζ_2. The idea here, is the simultaneous minimization of $|\Delta V'_{in}|$ and $|\Delta V_1|$ errors using ζ_1 and ζ_2, respectively.

$$V'_{in} = V_{in} - \zeta_1 . (V_{in} - V_i) \quad (26)$$

$$V_{1_{c+1}} = V_{1_c} + \zeta_2 \cdot \Delta V_1 \quad (27)$$

In other words, each dynamic damping factor works by suppressing undesired oscillations in voltage error vectors for VB ($|\Delta V_1|$) and for the rest system buses ($|\Delta V'_{in}|$). Unlike NBFS static damping, ζ_1 and ζ_2 are not fixed and could take upon any positive value within a specified range. The use of LF static damping factors is practiced in literature [9], [16]. However, as far as we know, most damping applications were based on trials of different damping values and fixing them for a particular set of LF problems. Moreover, it is very difficult to calculate ζ_1 and ζ_2 analytically [17], while attempting trial of different values is unpractical since many optimization problems that rely on LF is il-conditioned and using static damping will ultimately lead to solution divergence. Due to their impeccable record of solving non-convex and MINLP problems, metaheuristics have gained substantial interest and coverage in recent years [1]. Additionally, MIDACO is known for its high speed and precision when it comes to solving MINLP against other competitive swarm and evolutionary metaheuristics [4]. Therefore, MIDACO was adopted in GBFS to find and dynamically change ζ_1 and ζ_2 to minimize voltage error across the system. To ensure all DGs remain within their capacity, a reactive power correction vector γ_i was introduced to minimize the error in the reactive power error ΔQ_{Gi} at a generating bus i such that:

$$\Delta Q_{G1} \cdot n_{q1} + \gamma_1 = \Delta Q_{G2} \cdot n_{q2} + \gamma_2 = \Delta Q_{Gi} \cdot n_{qi} + \gamma_i \quad (28)$$

The value of γ_i can be analytically determined if prior knowledge exists about average reactive power in the IMG. Mathematically, γ_i as a function of DG reactive power and system average reactive power correction factor (Q_c) is [18], [19]:

$$\gamma_i = \left(\frac{Q_c}{\sum_{i \in \mathcal{GK}} \Delta Q_{Gi}} - 1\right) \cdot \{\Delta Q_{Gi}\} \cdot \beta \quad (29)$$

The value of Q_c is either communicated to DGs by the MGCC via low bandwidth communication channels or determined analytically as

$$Q_c = -(Q_{G1} - \Im\{V_1 \cdot B_1^*\}) \quad (30)$$

In case no DG unit is present at the VB, i.e. bus 1 in our study, then Q_{G1} should be set to zero. Also, since GBFS is based on minimal communication and to ensure reactive power correction is applied subsequently when any DG exceeds its power ratings, a binary constant is used in (27) and denoted as β:

$$\beta = \begin{cases} 0, & \forall\, Q_{min} < Q_{Gi} < Q_{max} \\ 1, & \forall\, Q_{Gi} \leq Q_{min}, Q_{Gi} \geq Q_{max} \end{cases} \quad (31)$$

Based on the forgoing, the reactive power reference Q_{Gi0} is corrected at each generating bus any time the reactive power output reaches the min-max ratings of the unit.

$$Q'_{Gi} = Q_{Gi0} + \gamma_i + Q_{Gi}\,;\ \forall\, i \in \mathcal{GK} \quad (32)$$

Similar to SBFS-II, GBFS also has one loop and converges when the condition E' is satisfied, i.e. $\mathrm{E}' < \varepsilon_{Th}$. A flow chart of the proposed two methods is depicted in Fig. 1.

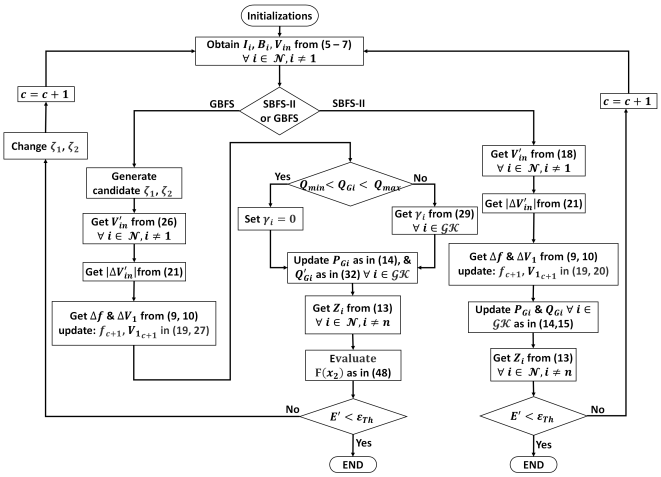

Fig 1. Flow chart of proposed SBFS-II and GBFS load flow methods

III. Optimization Problem Formulation

A. Proposed Optimization Method

The proposed optimization technique is based on the sophisticated MIDACO algorithm [20]. This high-performance solver is developed from ACOmi and OPM for constraint handling. The main ACO prototype in MIDACO is based on the extension of ACO to handle mixed-integer domains. This is achieved by having a multi-kernel gaussian probability density function (GPDF) rather than a pheromone table as the original ACO. This translates into three main parameters for single objective handling in MIDACO, viz. ANTS, KERNEL, and ORACLE [20]. Multi-objective handling on the other hand, is based on the utopia-nadir balance technique and multi-objective decomposition to single objective sub-problems each having j-th dimension. Accordingly, for a set $\mathbb{F}$ of feasible solutions, the utopia (U_i) is the so far best value of an objective function $\mathcal{F}_i(x)$, while the nadir (N_i) corresponds to the so far worst value compared to another utopia in the multi-objective domain [21].

$$U_i = min\{\mathcal{F}_i(x)\ \forall\, x \in \mathbb{F}\} \quad (33)$$

$$N_i = max\{\mathcal{F}_i(x)\ \forall\, x : \exists\, k \neq i : \mathcal{F}_k(x) = U_k\} \quad (34)$$

By having utopia-nadir of $\mathcal{F}_i(x)$, a scalar function for each sub-problem is introduced as balance function $B_j(x)$ [21].

$$B_j(x) = \sum_{i=1}^{M} \left| d_i^j(x) - D_j(x) \right| \quad (35)$$

where $d_i^j(x)$ and $D_j(x)$ are solution x weighted and average distances, respectively. And given by:

$$d_i^j(x) = w_i^j \cdot \left(\frac{f_i(x) - U_i}{N_i - U_i}\right) \quad (36)$$

$$D_j(x) = \frac{\sum_{i=1}^{M} d_i^j(x)}{M} \quad (37)$$

Based on that, a single objective function named, the target function $T_j(x)$, is used to solve each j-th sub-problem [21]:

$$T_j(x) = \sum_{i=1}^{M} d_i^j(x) + B_j(x) \quad (38)$$

The use of utopia-nadir balance concept is very beneficial in concentrating the search process on a promising area on the Pareto-front. This is incorporated in MIDACO as the BALANCE parameter to control the location of Pareto-front solution. To further enhance BALANCE, the algorithm employs the additional parameters EPSILON and PARETOMAX to dictate the rate and number of collected non-dominated solutions [20].

B. Dump Load Allocation Problem Formulation

The aim of the optimization problem in this paper is the optimal placement of DL using all three mentioned LF methods (SBFS, SBFS-II, and GBFS). The allocation is in terms of DL bus location (N_{DL}), active (P_{DL}) and reactive (Q_{DL}) DL size. Further, to select the optimal droop settings for dispatchable DGs that work best with the DL allocation. There are four objective functions in the multi-objective problem with a decision variable x_1 as follows:

$$\mathcal{F}_i(x_1) = min\{|\Delta V_1|, |\Delta f|, P_{loss}, Q_{loss}\} \quad (39)$$

$$x_1 = \{P_{DL}, Q_{DL}, mn_{DL}, N_{DL}\} \quad (40)$$

where $|\Delta V_1|$ and $|\Delta f|$ are V-f deviations, respectively, and obtained by minimizing the first step size for droop control P-f and Q-V curves as given in equations (1) and (2), respectively. This is advantageous, as the first response step has the biggest influence on droop control and the final settlement values for V-f. Moreover, the total active and reactive power losses in the IMG denoted, respectively, as P_{loss} and Q_{loss} are given by:

$$P_{loss} = \sum_{i=1}^{n-1} \Re\{Z_i\} \cdot |B_i|^2 \quad (41)$$

$$Q_{loss} = \sum_{i=1}^{n-1} \Im\{Z_i\} \cdot |B_i|^2 \quad (42)$$

On the other hand, the optimization problem was subjected to the following voltage, frequency, and line current constraints to ensure adequate IMG operation as per islanded systems guidance (per-unit system is used for all values with system base 12.66 KV, 500 KVA and $f_0 = 50\ Hz$) [4]:

$$0.95 \leq |V_i| \leq 1.05 \quad (43)$$

$$0.996 \leq f \leq 1.004 \quad (44)$$

$$|B_i| \leq |B_{i\_max}| \quad (45)$$

Furthermore, a DG and DL size limits were imposed as well as imposing a specified range for the optimal droop setting value for DL allocation (mn_{DL}) and is given by [4]:

$$mn_{DL} = m_{pi} = n_{qi} \quad (46)$$

$$10^{-4} \leq mn_{DL} \leq 1 \quad (47)$$

$$0 \leq \{P_{DG}, Q_{DG}\} \leq 2 \quad (48)$$

$$0.002 \leq \{P_{DL}, Q_{DL}\} \leq 1 \quad (49)$$

C. Damping Factors (ζ_1, ζ_2) Problem Formulation

As for GBFS optimization problem, a single objective formulation to achieve concurrent minimization of the two voltage error vectors $|\Delta V'_{in}|$ and $|\Delta V_1|$ is presented here. This is obtained by dynamically adjusting the damping factors ζ_1 and ζ_2 until convergence of GBFS. The choice of single objective approach over multi-objective formulation is well known to reduce calculation burden. By having a weighted average sum of the two objectives, i.e. $min\{|\Delta V'_{in}|, |\Delta V_1|\}$, the desired objective is achieved with minimal evaluation time. Despite the exploration and exploitation abilities provided by MIDACO, the pre-knowledge of the desired objective function value (i.e. ε_{Th}) will enable one of the most influential parameter by MIDACO for enhanced local search and increased speed. This is achieved by tuning the parameter FOCUS to a positive integer [20]. Moreover, to define the desired objective function value another parameter is initialized to equal ε_{Th}, that is the FSTOP parameter [20]. Based on the forgoing an additional decision variable is defined, denoted as x_2, to find the GBFS objective function:

$$\mathcal{F}(x_2) = \omega_1 \cdot max\{|\Delta V'_{in}|\} + \omega_2 \cdot |\Delta V_1|,\ x_2 = \{\zeta_1, \zeta_2\} \quad (48)$$

Where ω_1, ω_2 are weights between [0,1] for each objective. Noting that apart from setting sufficient limits for the damping factors $\zeta_1, \zeta_2 \in [0,10]$, a constraint handling in GBFS problem is not required.

TABLE I
DG UNITS DROOP SETS FOR DL BASE CASE, 33 BUS SYSTEM

DG Unit	DG_1	DG_2	DG_3	DG_4
Bus No.	1	6	13	25
m_{pi}	-0.05	-1	-0.1	-1
n_{qi}	-0.05	-1	-0.1	-1

TABLE II
GENERATION TO LOAD STATES 33 BUS SYSTEM

Load (%)	$\sum P_{Li}$ (p.u.)	$\sum Q_{Li}$ (p.u.)	Generation (%)	$\sum P_{Gi}$ (p.u.)	$\sum Q_{Gi}$ (p.u.)	Mismatch (%)
100	7.43	4.60	100	7.47	5.60	+6.84
50	3.72	2.30	63.63	4.20	4.20	+35.81

The off-peak hours scenario is represented by 50% peak system load.

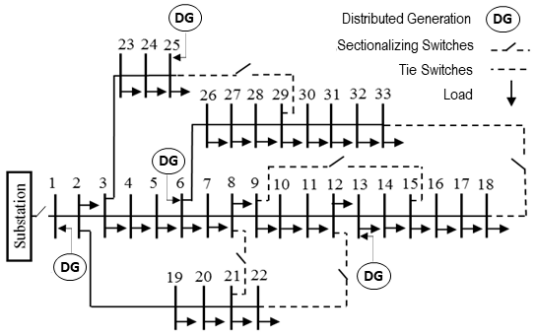

Fig 2. IEEE 33-bus system as prepared for islanding operation.

IV. RESULTS AND DISCUSSION

The IMG used to apply the DL optimization problem is IEEE-33 bus as depicted in Fig. 2. System line and load data are found in [22]. The test system and DL problem were built and simulated in MATLAB®. To mimic the significant mismatch in IMG, load demand was assumed to follow normal distribution where the highest probability is centred around the mean, that is around 50% demand drop during off-peak hours [23], [24]. The base case droop sets are given in Table I, while generation/loading states are given in Table II.

A. Multi-Objective Optimization

To simulate the many objectives problem in section III.B, MIDACO parameters were initialized as follows: BALANCE, PARETOMAX, and EPSILON were set to 0,1000, and 0.001, respectively, while zero was used for ANTS, KERNEL, and ORACLE. Hence, MIDACO will dynamically change the population in each generation using a sufficiently high oracle value. The pre-islanding apparent power of all units were assumed at $1.05 + j1.05$ p.u.. According to Table III results for the 33-bus system, the advantage of DL allocation was clear as the combination of MIDACO with all LF methods have managed to significantly reduce V-f to comply with IEEE std.1547.4 [25] as opposed to the base case (i.e. No DL using droop sets from Table I). Furthermore, despite the significant DL size the incurred losses by such application were reduced to almost match the base case. Additionally, adopting SBFS-II as LF method within MIDACO, has improved the calculation time by 6 seconds if compared to SBFS-based solution. Nonetheless, the accuracy of the optimization method did not deviate from obtaining almost identical objective function values for both SBFS and SBFS-II. On the other hand, using GBFS with MIDACO has significantly improved the accuracy of the DL allocation with increased calculation time. As given in Table

TABLE III
MULTI-OBJECTIVE DL RESULTS USING DIFFERENT LF, 33 BUS SYSTEM

LF Method	SBFS		SBFS-II		GBFS	
Case	No DL	w/DL	No DL	w/DL	No DL	w/DL
N_{DL}	-	13	-	13	-	13
P_{DL} (p.u.)	-	0.2319	-	0.2377	-	0.3399
Q_{DL} (p.u.)	-	0.1594	-	0.1752	-	0.7282
mn_{DL} (p.u.)	-	0.0191	-	0.0188	-	0.0053
$\lvert\Delta V_1\rvert$ (p.u.)	0.0586	0.0082	0.0586	0.0080	0.0586	0.0015
$\lvert\Delta f\rvert$ (p.u.)	0.0141	0.0011	0.0141	0.0011	0.0141	0.0002
P_{loss} (p.u.)	0.0195	0.0201	0.0195	0.0202	0.0194	0.0197
Q_{loss} (p.u.)	0.0153	0.0154	0.0153	0.0154	0.0152	0.0151
MVE (p.u.)	0.0642	0.0119	0.0642	0.0121	0.0628	0.0189
f_{ss} (p.u.)	1.0145	1.0011	1.0145	1.0012	1.0146	1.0002
Time (s)	-	41	-	35	-	95

First step size only for $|\Delta V_1|$ and $|\Delta f|$. MVE: maximum voltage error, f_{ss}: steady state frequency.

TABLE IV
DL CONVERGENCE TESTS (1A-4A) & LF CALCULATION TIME IN SECONDS

Convergence Test		1A[a]	2A	3A	4A[b]
N_{DL}		-	13	13	1
mn_{DL}		-	0.2377	0.3399	0.0046
P_{DL} (p.u.)		-	0.1752	0.7282	0.0032
Q_{DL} (p.u.)		-	0.0188	0.0053	0.0125
Load Flow Method & Time (s)	DBFS	0.0160	NC	NC	NC
	SBFS	0.0063	0.0054	0.0059	0.0061
	SBFS-II	0.0044	0.0036	0.0038	0.0040
	MBFS	0.0187	NC	NC	NC
	NBFS	0.0181	NC	NC	NC
	GBFS	0.0074	0.0059	0.0065	0.0112

[a]Using droop values from Table I, [b]Refers to random generated solution by MIDACO within first 100 evaluations, NC: Not Converged.

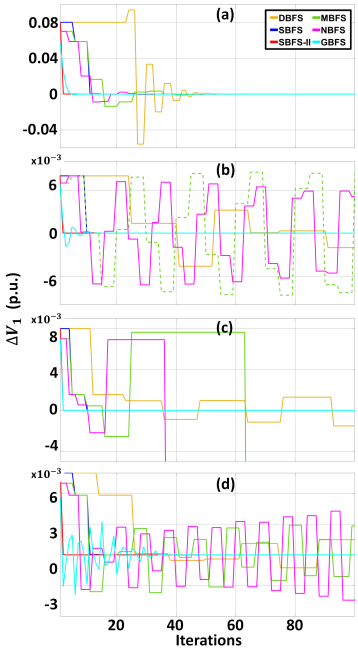

Fig 3. Convergence of ΔV_1 for 33-bus (a) Test 1A (b) Test 2A (c) Test 3A (d) Test 4A

III, the optimized V - f deviations were much lower as opposed to SBFS- and SBFS-II-based solutions. Conversely, although GBFS has increased the size of DL the obtained losses were slightly lower than those of SBFS and SBFS-II. This is attributed to the advantage of local voltage measurement by GBFS against global voltage distribution approach. Since the generated power by DGs will be increased unnecessarily to match a remote bus voltage. What worth noting here as well, is the reduced Q_{loss} obtained if compared to the No DL case. This can be explained by having an inductive reactive compensation in a highly capacitive network caused by the significant over-generation reactive power mismatch.

TABLE V
DG UNITS DROOP GAINS 33 BUS SYSTEM FOR LF TEST (FULL LOAD)

DG Unit	*Bus No.*	Test (1B,1C)		Test (2B,2C)		Test (3B,3C)		Test (4B,4C)	
		m_{pi}	n_{qi}	m_{pi}	n_{qi}	m_{pi}	n_{qi}	m_{pi}	n_{qi}
DG_1	1	-0.05	**-0.05**	-0.016	**-0.016**	-0.002	**-0.009**	-0.001	**-0.004**
DG_2	6	-1	**-1**	-0.016	**-0.016**	-0.003	**-0.03**	-0.0014	**-0.014**
DG_3	13	-0.1	**-0.1**	-0.016	**-0.016**	-0.003	**-0.015**	-0.0014	**-0.014**
DG_4	25	-1	**-1**	-0.016	**-0.016**	-0.004	**-0.03**	-0.0014	**-0.014**
DG_5	33	-0.2	**-0.2**	-0.016	**-0.016**	-0.008	**-0.015**	-0.0014	**-0.014**

TABLE VI
LF ITERATIONS USING INDUCTIVE DROOP RESPONSE, 33-BUS SYSTEM

Test	LF Method				
	MBFS	NBFS	GBFS		
	Iterations			ζ_1	ζ_2
1B	62	29	5	0.6299	0.8667
2B	NC	NC	86	2.6396	1.9720
3B	NC	NC	60	0.4552	1.9958
4B	NC	NC	66	2.8848	2.0929

NC: Not Converged.

TABLE VII
LF ITERATIONS USING COMPLEX DROOP RESPONSE, 33-BUS SYSTEM

Test	LF Method				
	MBFS	NBFS	GBFS		
	Iterations			ζ_1	ζ_2
1C	468	279	40	0.1331	0.3004
2C	NC	NC	42	9.9158	3.1934
3C	NC	NC	64	9.8912	4.2152
4C	NC	NC	34	3.2531	4.1295

NC: Not Converged.

B. *Convergence of SBFS-II and GBFS*

Convergence of the proposed two LF methods was tested using DL solutions as obtained in Table III. Four convergence tests (1A-4A) considering DL allocation scenario at off-peak hours were given in Table IV, while ΔV_1 convergence curves over 100 iterations for different LF methods is illustrated in Fig. 3 (all convergence tests in this paper were subjected to $\varepsilon_{Th} = 10^{-8}$ for all LF methods). According to ΔV_1 graphs, SBFS-II holds the best convergence response followed by SBFS and GBFS. This can be explained by having a global voltage variable dictating the reactive power update in SBFS and SBFS-II methods, this has generally much faster convergence response than local voltage reactive power updates in GBFS. Likewise, time of LF solution considering DL values using the different LF methods is given in Table IV. As expected SBFS-II has a very quick response if compared to the rest of the methods, while GBFS had a very acceptable calculation times if it was compared with MBFS and NBFS. Noting that the latter two LF methods failed to convergence on different tests.

To further validate the robustness of GBFS against other local voltage-based IMG solution, additional convergence tests were considered using different variations for droop equations. Wherein inductive and complex DG output impedance was considered in tests (1B-4B) and (1C-4C), respectively. Moreover, tests were performed using a full loaded 33-bus system with an additional DG unit installed at bus no. 33 as considered by [8]. For a fair comparison, all DG units were assumed with pre-islanding generation as $0.9 + j0.9$ p.u. and no DL was considered [8]. Droop gains considered for convergence tests 1B to 4C are given in Table V. The number of iteration required to obtaine a converged LF solution by MBFS, NBFS, and GBFS considering inductive and complex droop response are given in Tables VI and VII, respectively. As can be seen from the results, both MBFS and NBFS have failed to converge with lower droop

selection, while GBFS has lower number of iterations if compared to MBFS and NBFS for both tests 1B and 1C.

V. Conclusion

In this paper, two LF methods, SBFS-II and GBFS, were proposed with MIDACO to improve the multi-objective DL allocation problem in DCIMG. The former LF method relies on global voltage value distributed between DGs with one loop, while GBFS utilizes two dynamic damping factors ζ_1 and ζ_2 to suppress voltage error across the system. Moreover, the introduction of a reactive power correction vector γ_i by GBFS to keep DGs within power limits. The benefit of the two LF methods were validated on IEEE 33-bus system, with the results showing faster calculation times and better convergence response for SBFS-II over SBFS. While GBFS has demonstrated higher accuracy over SBFS with acceptable convergence and calculation speeds in the DL allocation problem. Lastly, the decision to use any of the proposed LF methods is based on accuracy and speed requirements for any optimization problem at the planning stage of DCIMG. Wherein SBFS-II offers very fast but approximate solution while GBFS has more accurate but relatively slower solution.

References

[1] M. Z. Kreishan and A. F. Zobaa, "Optimal Allocation and Operation of Droop-Controlled Islanded Microgrids: A Review," *Energies*, vol. 14, no. 15, Art. no. 15, Jan. 2021.

[2] A. Uniyal and S. Sarangi, "Optimal allocation of ELC in microgrid using droop controlled load flow," *Transmission Distribution IET Generation*, vol. 13, no. 20, pp. 4566–4578, Oct. 2019.

[3] A. Uniyal, S. Sarangi, and M. S. Rawat, "Optimal Dump Load Allocations in High RBDG Penetrated Microgrid for Voltage and Frequency Regulation," *Arab J Sci Eng*, vol. 46, no. 2, pp. 1511–1528, Feb. 2021.

[4] M. Z. Kreishan and A. F. Zobaa, "Allocation of Dump Load in Islanded Microgrid Using the Mixed-Integer Distributed Ant Colony Optimization," *IEEE Systems Journal*, pp. 1–12, 2021.

[5] D. Shirmohammadi, H. W. Hong, A. Semlyen, and G. X. Luo, "A compensation-based power flow method for weakly meshed distribution and transmission networks," *IEEE Transactions on Power Systems*, vol. 3, no. 2, pp. 753–762, May 1988.

[6] A. Dukpa, B. Venkatesh, and M. El-Hawary, "Application of continuation power flow method in radial distribution systems," *Electric Power Systems Research*, vol. 79, no. 11, pp. 1503–1510, Nov. 2009.

[7] G. Díaz, J. Gómez-Aleixandre, and J. Coto, "Direct Backward/Forward Sweep Algorithm for Solving Load Power Flows in AC Droop-Regulated Microgrids," *IEEE Transactions on Smart Grid*, vol. 7, no. 5, pp. 2208–2217, Sep. 2016.

[8] F. Hameed, M. Al Hosani, and H. H. Zeineldin, "A Modified Backward/Forward Sweep Load Flow Method for Islanded Radial Microgrids," *IEEE Transactions on Smart Grid*, vol. 10, no. 1, pp. 910–918, Jan. 2019.

[9] A. Kumar, B. K. Jha, D. K. Dheer, D. Singh, and R. K. Misra, "Nested backward/forward sweep algorithm for power flow analysis of droop regulated islanded microgrids," *Transmission Distribution IET Generation*, vol. 13, no. 14, pp. 3086–3095, Jul. 2019.

[10] M. Schlüter, J. A. Egea, and J. R. Banga, "Extended ant colony optimization for non-convex mixed integer nonlinear programming," *Computers & Operations Research*, vol. 36, no. 7, pp. 2217–2229, Jul. 2009.

[11] M. Schlüter and M. Gerdts, "The oracle penalty method," *J Glob Optim*, vol. 47, no. 2, pp. 293–325, Jun. 2010.

[12] M. Schlueter, C. H. Yam, T. Watanabe, and A. Oyama, "Many-objective optimization of interplanetary space mission trajectories," in *Proc. IEEE CEC*, Sendai, Japan, 2015, pp. 3256–3262.

[13] "IEEE Guide for Conducting Distribution Impact Studies for Distributed Resource Interconnection," *IEEE Std 1547.7-2013*, pp. 1–137, Feb. 2014.

[14] F. Mumtaz, M. H. Syed, M. A. Hosani, and H. H. Zeineldin, "A Novel Approach to Solve Power Flow for Islanded Microgrids Using Modified Newton Raphson With Droop Control of DG," *IEEE Transactions on Sustainable Energy*, vol. 7, no. 2, pp. 493–503, Apr. 2016.

[15] Jen-Hao Teng, "A direct approach for distribution system load flow solutions," *IEEE Transactions on Power Delivery*, vol. 18, no. 3, pp. 882–887, Jul. 2003.

[16] P. J. Lagace, M. H. Vuong, and I. Kamwa, "Improving power flow convergence by Newton Raphson with a Levenberg-Marquardt method," in *Proc. IEEE PESGM - CDEE 21st Century*, Jul. 2008, pp. 1–6.

[17] A. Elrayyah, Y. Sozer, and M. E. Elbuluk, "A Novel Load-Flow Analysis for Stable and Optimized Microgrid Operation," *IEEE Transactions on Power Delivery*, vol. 29, no. 4, pp. 1709–1717, Aug. 2014.

[18] Y. Han, H. Li, P. Shen, E. A. A. Coelho, and J. M. Guerrero, "Review of Active and Reactive Power Sharing Strategies in Hierarchical Controlled Microgrids," *IEEE Transactions on Power Electronics*, vol. 32, no. 3, pp. 2427–2451, Mar. 2017.

[19] Y. Zhu, F. Zhuo, and H. Shi, "Accurate power sharing strategy for complex microgrid based on droop control method," in *Proc. IEEE ECCE Asia Downunder*, Melbourne, VIC, Australia, 2013, pp. 344–350.

[20] M. Schlueter and M. Munetomo, "MIDACO solver user manual 6.0," Hokkaido University, Sapporo, Japan, Technical Report, 2018. [Online]. Available: http://www.midaco-solver.com/data/other/MIDACO_User_Manual.pdf.

[21] M. Schlueter, C. H. Yam, T. Watanabe, and A. Oyama, "Parallelization impact on many-objective optimization for space trajectory design," *International Journal of Machine Learning and Computing*, vol. 6, no. 1, pp. 9–14, Feb. 2016.

[22] M. E. Baran and F. F. Wu, "Network reconfiguration in distribution systems for loss reduction and load balancing," *IEEE Transactions on Power Delivery*, vol. 4, no. 2, pp. 1401–1407, Apr. 1989.

[23] Y. M. Atwa and E. F. El-Saadany, "Probabilistic approach for optimal allocation of wind-based distributed generation in distribution systems," *IET Renewable Power Generation*, vol. 5, no. 1, pp. 79–88, Jan. 2011.

[24] E. Hajipour, M. Bozorg, and M. Fotuhi-Firuzabad, "Stochastic Capacity Expansion Planning of Remote Microgrids With Wind Farms and Energy Storage," *IEEE Transactions on Sustainable Energy*, vol. 6, no. 2, pp. 491–498, Apr. 2015.

[25] "IEEE Guide for Design, Operation, and Integration of Distributed Resource Island Systems with Electric Power Systems," *IEEE Std 1547.4-2011*, pp. 1–54, Jul. 2011.